V.G. Dan'ko, E.V. Goncharov, I.V. Poliakov

# ANALYSIS OF THE OPERATION PECULIARITIES OF THE SUPERCONDUCTING INDUCTIVE CURRENT LIMITER WITH ADDITIONAL SUPERCONDUCTING SCREEN

*Purpose. The inductances of magnetic system of a current limiter for the nominal operating mode were determined. The aspects of functioning and a design of a superconducting short-circuit current limiter of inductive type with a superconductive main and additional screens, and superconductive winding, which are placed in a general cryostat on a ferromagnetic core, which ensures an improvement of magnetic field dissipation and in energy efficiency are observed. Methodology. The analysis of distribution of magnetic field of the short-circuit current limiter of inductive type with superconducting high-temperature coil and superconducting main and additional screens, using mathematical modeling by the finite element method in math software package FEMM for different modes of operation is carried out. Results. The calculations of magnetic field dissipation in operational modes are carried out. Originality. The investigations aimed to analyze the influence of distribution of the magnetic field in inductive short-circuit current limiter with superconducting additional screen on its operation modes. First calculation of the distribution of magnetic fields in different modes of operation for the short-circuit current limiter in the area between high-temperature superconducting screens. Practical value. The advantage of additional screen of superconducting short-circuit current limiter is to improve screening from dissipation of the magnetic fields of the magnetic system and reducing the power losses at nominal mode. Using the proposed methodology will identify options acceptable to the current limiter mode of operation.* References 15, tables 3, figures 6.
*Key words:* **current limiter, high-temperature superconductor, superconducting screen, inductance, magnetic field, ferromagnetic core**.

*Проведен анализ режимов работы и конструктивной схемы сверхпроводящего ограничителя тока короткого замыкания индуктивного типа с дополнительным сверхпроводящим экраном. Проведено математическое моделирование магнитной системы ограничителя тока методом конечных элементов в программной среде FEMM. Проведен расчет распределения магнитных полей в различных режимах срабатывания ограничителя тока короткого замыкания на участке между основным и дополнительным экранами, что позволяет определить параметры ограничителя тока.* Библ. 15, табл. 3, рис. 6.
*Ключевые слова:* **ограничитель тока, высокотемпературный сверхпроводник, сверхпроводящий экран, индуктивность, магнитное поле, магнитопровод**.

**Introduction.** The development of the electric power industry is characterized by an increase in the generation of electricity, the development of increased capacities, the creation of high-power power systems. Thus, there were prerequisites for the development of electric power on a new technological basis of high-temperature superconductivity.

A superconducting high-temperature short-circuit current limiter is an alternative to the use of conventional current-limiting reactors. According to the structural features, two main concepts of the superconducting current limiter can be distinguished: resistive and inductive, and other circuitry based on them [1, 2].

The resistive design of the superconducting current limiter, based on the nonlinearity of the superconductor's resistance, can use massive elements or coils [3]. In the case of superconducting coils utilization as superconducting elements, they are connected so that the full inductance of the limiter is minimal [4]. The main disadvantage of a resistive superconducting current limiter is significant heat dissipation and overheating at short circuits.

In the inductive construction, which is considered in the work of Yonsei University, the magnetic coupling between the superconducting element and the winding is carried out through the three-rod magnet [5]. Also, for example, in the work of the ABB Company a three-phase current limiter (1.2 MVA) with a cylindrical screen of 16

rings of superconducting ceramics Bi-2212 has been designed, which was tested and operated during the year [6]. The operation of an inductive current limiter is due to the presence of magnetic scattering fields, which can negatively affect the use of a metal cryostat and increase power losses.

Reducing the effect of magnetic scattering fields can be achieved by using an additional superconducting screen.

But the features of the inductive current limiter, using an additional superconducting screen, have not been investigated.

**The goal and definition of the research.** The goal of the paper is to investigate the features of the short circuit current limiter with an additional superconducting screen. The purpose of the work is to analyze the modes of operation with the definition of the distribution of magnetic fields in the current limiter.

The general view of the design scheme of the current limiter with the additional superconducting screen and the circuit for switching on the phase of the mains with the load is given in Fig. 1 [7].

The short-circuit current limiter is located in the cryostat *1* with the current conductors *2* on the middle rod of the ferromagnetic core of the magnetic circuit *3*. From the inner wall of the cryostat to the outer axially the main superconducting screen *4*, the outer superconducting

screen *5*, the superconducting coil *6* between them are located. The cryostat is filled with liquid nitrogen for cooling the winding and screens to the superconducting state (77 K) [8].
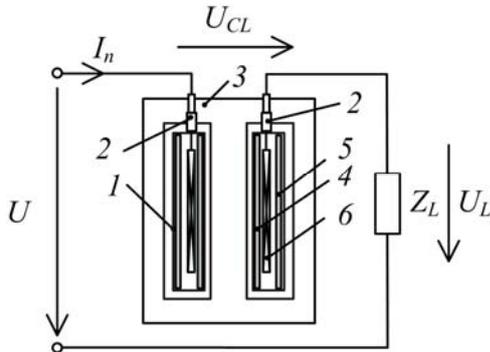


Fig. 1. Design scheme of the current limiter

The winding *6* is connected in series with the load, and in the nominal mode through it the load current $I_n$ flows. The superconducting screen *4* shields the middle magnet circuit rod from the magnetic field that is created by the winding *6*.

Inductance of the superconducting current limiter winding at nominal mode [9]:

$$L_{sc} = \frac{\Psi}{I_n} = \mu_a w^2 \frac{2\pi \, r_{mid} b}{3h_{coil}},$$

where $\Psi$ is the winding flux linkage; $I_n$ is the rated current; $r_{mid}$ is the average winding radius; $b$ is the winding width; $h_{coil}$ is the winding height; $w$ is the winding number of turns; $\mu_a$ is the absolute magnetic permeability [10].

Let us consider how the voltage drop $U_{CL}$ on the current limiter affects the load voltage decrease $U_L$ in relation to the voltage of the electrical network $U$. The use of high-temperature superconductors for the windings of the current limiter reduces their resistance to practically purely inductive ($R \to 0$). That is, the voltage on the current limiter $U_{CL}$ outstrips the current $I_n$ by $\sim 90°$ (Fig. 2).
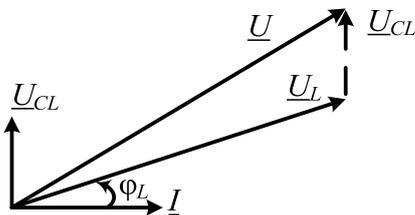


Fig. 2. Vector diagram of the electric circuit with superconducting current limiter

According to the vector diagram $\underline{U} = \underline{U}_L + \underline{U}_{CL} = \underline{U}_L + k_{CL}\underline{U}_L$, where $k_{CL}$ is the correlation coefficient $U_{CL}$ with load voltage $U_L$.

From the vector diagram, the load voltage

$$U_L = \frac{U}{\sqrt{\left(k_{CL} + \sqrt{1 - \cos^2 \varphi_L}\right) + \cos^2 \varphi_L}},$$

where $\varphi_L$ is the angle of the phase shift of the nature of the load.

In industrial regions of Ukraine, $\cos\varphi$ is within the range of 0.9-0.95, therefore the voltage on the current limiter should be limited to $0.05U_L$, laying the appropriate design parameters of the current limiter [11]. With $\cos\varphi \approx 0.97$, one can accept $k_{CL} = (0.1\text{-}0.15)$. The results of the calculation of the relationship between the load voltage $U_L$ and the voltage of the electrical network $U$, depending on $k_{CL}$ and $\cos\varphi_L$ are shown in Table 1.

Table 1

$U_L$ as a part of $U$

| $k_{CL}$ | $\cos\varphi_L$ | | | |
|---|---|---|---|---|
| | 0.85 | 0.9 | 0.95 | 1.0 |
| 0.05 | 0.973 *U* | 0.977 *U* | 0.983 *U* | 0.999 *U* |
| 0.1 | 0.947 *U* | 0.954 *U* | 0.965 *U* | 0.995 *U* |
| 0.15 | 0.92 *U* | 0.931 *U* | 0.946 *U* | 0.99 *U* |

From Table 1 it is evident that with an active load of the electric network, the superconducting current limiter, even with a significant drop in the voltage on it, practically does not affect the voltage decrease on the load.

**Calculation of the magnetic field distribution.** The calculation of the distribution of the magnetic field in the nominal mode of the current limiter operation using the finite element method in the FEMM mathematical software package [12] was carried out.

To calculate the magnetic field, a calculation geometric model of the magnetic system of the current limiter was built with the parameters given in Table 2 [13].

Table 2

Current limiter parameters

| Parameter | Value |
|---|---|
| Rated voltage, kV | 6 |
| Rated current, A | 400 |
| Radius of the core section $r_c$, m | 0.105 |
| Magnetic circuit width $A$, m | 0.471 |
| Height of the magnetic core window $h$, m | 0.84 |
| Superconducting screens height $h_{scr}$, m | 0.82 |
| Winding height $h_{coil}$, m | 0.81 |
| Winding number of turns $w$ | 367 |
| Gap between the main screen and winding $\delta_{scr}$, mm | 1-5 |

The distribution of the magnetic field in the window of the magnetic core of the current limiter at the nominal mode, which is calculated in the FEMM package, is shown in Fig. 3.

The geometric model of the limiter magnetic circuit is built in FEMM for inductance calculations with the assumption that the cross-section of the current limiter is rectangular and the distribution of the magnetic flux does not change in radial direction [14].

Calculation of the inductive resistance of the equivalent model of the current limiter in nominal mode is performed on the basis of the calculation of the magnetic field and is shown in Table 3.
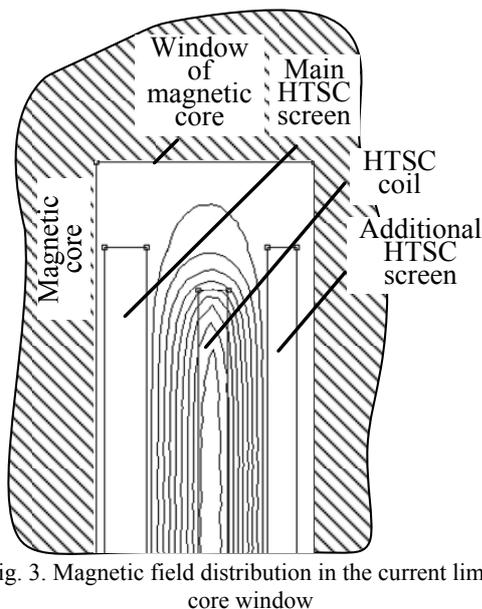
Fig. 3. Magnetic field distribution in the current limiter core window
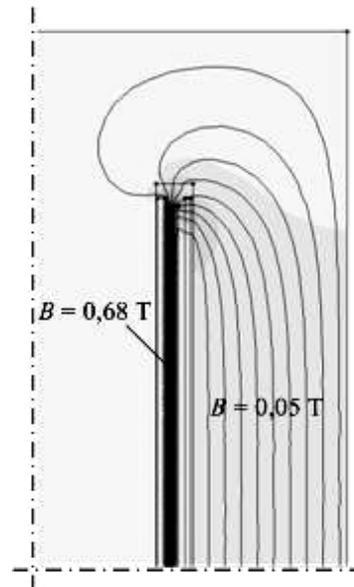


Fig. 4. Distribution of the magnetic field at the loss of superconductivity by additional screen

Table 3

Inductive resistance $X_L$ at $\mu_r = 1$

| $\delta_{scr}/h_{coil}$, % | $X_L$, $\Omega$ | $k_{CL}$ |
|---|---|---|
| 0.1 | 0.0917 | $6.11 \cdot 10^{-03}$ |
| 0.2 | 0.129 | $8.61 \cdot 10^{-03}$ |
| 0.3 | 0.165 | $1.10 \cdot 10^{-02}$ |
| 0.4 | 0.199 | $1.32 \cdot 10^{-02}$ |
| 0.5 | 0.239 | $1.59 \cdot 10^{-02}$ |

The inductance of the winding due to the magnetic fluxes of scattering, taking into account shielding, is negligible. The full resistance of this current limiter at the rated operating mode of the power supply is small enough, which does not lead to a significant reduction in the voltage on the load $U_{CL} < 3$ % of $U$, and the nature of the voltage drop is inductive.

In the nominal mode of operation, an additional superconducting screen provides the passage of magnetic flux outside of the winding. Magnetic scattering fields the outside of the winding are shielded by an additional superconducting screen. The magnetic flux does not penetrate the extreme magnetic circuit bars, therefore, the losses in the magnetic circuit are not present at the nominal mode. The transient process at the operation of a screened superconducting current limiter can take place in several stages.

There are two options for operating the current limiter with an additional screen. In the case of loss of superconductivity by an additional superconducting screen at the critical magnetic field strength $H_{cr}$, when the current in the winding reaches the value $I_{cr1} = 3I_n$, the inductance of the winding is $L = 0.3$ mH. The magnetic flux extends from the outside of the surface of the main superconducting screen and penetrates the extreme bars of the magnetic circuit. The calculation of the distribution of the magnetic field of the winding with $\mu_r = 1$ is presented in Fig. 4.

In the case of loss of superconductivity by additional screen, the magnetic flux extends along the area belonging to the window of the section of the magnetic core and forms the flux linkage, but this is not sufficient to provide a limiting short-circuit current. With the subsequent loss of the superconductivity of the main screen after the loss of superconductivity by the additional one, the inertial component and scattering fields will take place. The distribution of magnetic flux density $B$ along the area from the outer wall of the main superconducting screen to the inner wall of the additional screen, which has lost the superconducting properties, is given in the graph in Fig. 5.
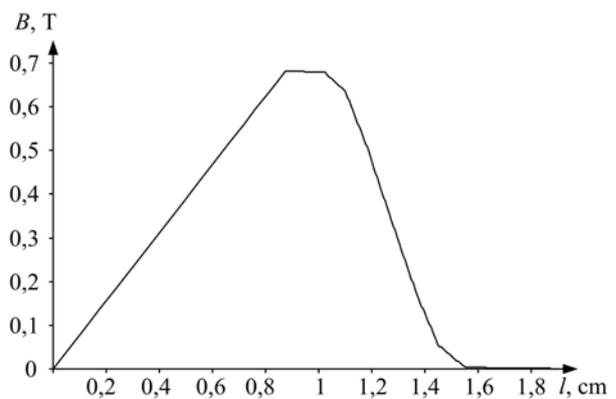


Fig. 5. Distribution of the magnetic flux density between the screens

In this case, the magnetic flux density has the maximal value in the middle section of the superconducting winding.

For example, in case of loss of superconductivity by the main screen, provided $I_{cr2} = 3I_n$, the critical parameters of the main screen should be lower than for the additional screen $H_{cr1}(I_{cr1}) < H_{cr2}(I_{cr2})$. The magnetic flux of scattering is sprayed in the window of the magnetic core, but only penetrates the middle bar of the magnetic circuit core, except the extreme (axial

symmetry). The calculation of the distribution of the magnetic field is given in Fig. 6, the inductance of the winding in this case is $L = 0.24$ mH.
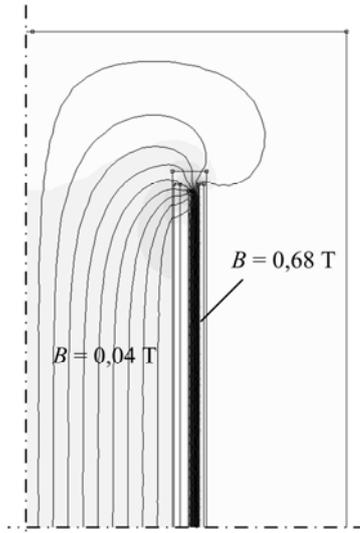


Fig. 6. Distribution of the magnetic field at the loss
of superconductivity by main screen

The distribution of magnetic flux density in the area between the screens will be similar, with the difference that the magnetic scattering flux goes away the winding from the outside at the extreme bar.

When the current in the coil reaches the critical value corresponding to the main and additional screens $I_{cr1} = I_{cr2} = 3I_n$, simultaneous loss of their superconductivity will occur. The magnetic flux instantly penetrates the middle bar of the magnetic circuit, the inductance increases, which provides a current limitation and increases the time constant of increase of current, which in general will facilitate the switch operation. The transient will take place in two stages. In this case, the mathematical model of the transient is determined by the equations [15]:

$$
\begin{cases}
i_{cr1}(t) = \dfrac{U_{nm}}{Z_{CL1}}\sin(\omega t + \psi_u - \varphi_{CL1}) + \\
+ \left[ I_{nm}\sin(\psi_u - \varphi_L) - \dfrac{U_{nm}}{Z_{CL1}}\sin(\psi_u - \varphi_{CL1}) \right] e^{-\frac{R_{CL1}}{L_{CL1}}t} ; \\
i_{cr2}(t) = \dfrac{U_{nm}}{Z_{CL2}}\sin[\omega(t + t_{cr1}) + \psi_u - \varphi_{CL2}] + \\
+ \left[ k_{i1}I_{nm} - \dfrac{U_{nm}}{Z_{CL2}}\sin(\omega t_{cr1} + \psi_u - \varphi_{CL2}) \right] e^{-\frac{R_{CL2}}{L_{CL2}}t} ;
\end{cases}
$$

where $R_{CL1} = R_{CL2} = P_0/I_n^2$ is the winding resistive resistance; $P_0$ is the winding power losses;

$$ L_{CL1} = \mu_0 n^2 w \frac{b_w}{a_w}\pi r_c , \qquad L_{CL2} = \frac{w B_c \pi r_c^2}{k_{i1}I_{nm}} \qquad \text{are the} $$

inductances of the current limiter of the first and the second stages; $w$ is the winding number of turns; $a_w$ is the film wire width; $b_w$ is the film wire thickness; $r_c$ is the radius of the magnetic circuit core section; $B_c$ is the

magnetic flux density of the core; $t_{cr1}$ is the time of the end of the first stage of the transient;

$$ Z_{CL1} = \sqrt{R_{CL1}^2 + (\omega L_{CL1})^2} , \quad Z_{CL2} = \sqrt{R_{CL2}^2 + (\omega L_{CL2})^2} $$

are the impedances of the current limiter of the first and the second stage; $\varphi_{CL1} = \text{arctg}\dfrac{\omega L_{CL1}}{R_{CL1}}$,

$\varphi_{CL2} = \text{arctg}\dfrac{\omega L_{CL2}}{R_{CL2}}$ are the phase angles of the current

limiter of the first and the second stages; $k_{i1} = 2.5\text{-}3$ is the current excess ratio.

**Conclusions.** The use of an additional superconducting screen in an inductive current limiter provides shielding of magnetic scattering fields thereby the heat flux and power losses in nominal mode reduce, although the use of an additional superconducting screen slightly increases the core mass of the magnetic circuit.

Analysis of the distribution of the magnetic field shows that the variant of operation of the current limiter at the moment of short circuit is more suitable at the primary loss of superconductivity of the main screen, which makes it advisable for it to use material with lower critical parameters, for example, bismuth ceramics, and for the additional screen to use yttrium ceramics.

REFERENCES
*1.* Leung E.M. Superconducting fault current limiters. *IEEE Power Engineering Review*, 2000, vol.20, no.8, pp. 15-18. **doi: 10.1109/39.857449.**
*2.* Paul W., Chen M., Lakner M., Rhyner J., Braun D., Lanz W. Fault current limiter based on high temperature superconductors − different concepts, test results, simulations, applications. *Physica C: Superconductivity*, 2001, vol.354, no.1-4, pp. 27-33. **doi: 10.1016/s0921-4534(01)00018-1.**
*3.* Bock J., Breuer F., Walter H., Elschner S., Kleimaier M., Kreutz R., Noe M. CURL 10: development and field-test of a 10 kV/10 MVA resistive current limiter based on bulk MCP-BSCCO 2212. *IEEE Transactions on Applied Superconductivity*, 2005, vol.15, no.2, pp. 1955-1960. **doi: 10.1109/tasc.2005.849344.**
*4.* Elschner S., Breuer F., Noe M., Rettelbach T., Walter H., Bock J. Manufacturing and testing of MCP 2212 bifilar coils for a 10 MVA fault current limiter. *IEEE Transactions on Applied Superconductivity*, 2003, vol.13, no.2, pp. 1980-1983. **doi: 10.1109/tasc.2003.812954.**
*5.* Joo M. Reduction of fault current peak in an inductive high-Tc superconducting fault current limiter. *Cryogenics*, 2005, vol.45, no.5, pp. 343-347. **doi: 10.1016/j.cryogenics.2004.11.007.**
*6.* Paul W., Chen M., Lakner M., Rhyner J., Widenhorn L., Guérig A. Test of 1.2 MVA high-Tc superconducting fault current limiter. *Superconductor Science and Technology*, 1997, vol.10, no.12, pp. 914-918. **doi: 10.1007/978-4-431-66879-4_292.**
*7.* Goncharov E.V. *Strumoobmezhuyuchyy reaktor z nadprovidnym kombinovanym ekranom* [Superconducting current-limiting reactor combined screen]. Patent UA, no. 112671, 2016. (Ukr).
*8.* Goncharov E.V. Improving shielding of superconducting inductively resistive short-circuit current limiter. *Materialy nauk.-tekhn. konf «Problemy suchasnoi enerhetyky i avtomatyky v systemi pryrodokorystuvannia».* [Abstracts of Sci.-Techn. Conf. «Problems of modern energy and automation system of nature»]. Kyiv, 14-18 November 2016, pp. 107-108. (Ukr).

*9.* Dan'ko V.G., Goncharov E.V. Analysis of high-temperature superconducting short-circuit current limiter. *Eastern-European Journal of Enterprise Technologies*, 2007, vol.6/5(30), pp. 45-48. (Ukr).

*10.* Goncharov E.V. Equivalent magnetic permeability of superconducting winding. *Electrical engineering & electromechanics*, 2010, no.1, pp. 11-13. (Ukr). **doi: 10.20998/2074-272X.2010.1.03.**

*11.* Dan'ko V.G., Goncharov E.V. Calculating the parameters of an inductive short-circuit current limiter with a superconducting shield. *Russian Electrical Engineering*, 2013, vol.84, no.9, pp. 478-481. **doi: 10.3103/s1068371213090046.**

*12.* Meeker D. *Finite Element Method Magnetics. FEMM 4.2 32 bit 11 Oct 2010 Self-Installing Executable.* Available at: www.femm.info/wiki/OldVersions (accessed 10 March 2014).

*13.* Dan'ko V.G., Goncharov E.V., Polyakov I.V. Analysis of energy efficiency of a superconducting short circuit current limiter. *Eastern-European Journal of Enterprise Technologies*, 2016, vol.6, no.5(84), pp. 4-12. **doi: 10.15587/1729-4061.2016.84169.**

*14.* Dan'ko V.G., Goncharov E.V. Synthesis aspects of cryogenic high-temperature superconducting shielding inductive short-circuit current limiter. *Bulletin of NTU «KhPI»*, 2016, no.32(1204), pp. 3-7.

*15.* Dan'ko V.G., Goncharov E.V. Features of operation of a superconducting current limiter at the sudden short circuit. *Electrical engineering & electromechanics*, 2014, no.6, pp. 30-33. (Ukr). **doi: 10.20998/2074-272X.2014.6.04.**

*V.G. Dan'ko*[1], *Doctor of Technical Science, Professor,*
*E.V. Goncharov*[1], *Candidate of Technical Science,*
*I.V. Poliakov*[1], *Candidate of Technical Science, Associate Professor,*
[1] National Technical University «Kharkiv Polytechnic Institute»,
2, Kyrpychova Str., Kharkiv, 61002, Ukraine,
phone +380 57 7076427,
e-mail: e.goncharov.v@gmail.com